Calculation of Transonic Flows by a Field Integral Equation Method

C. P. Chen* and M. J. Sheu†
National Tsing Hua University, Hsinchu, Taiwan, Republic of China

A field integral equation method is developed to solve the two-dimensional compressible potential equation for transonic flow over airfoils with embedded shocks at subsonic freestream Mach numbers. The perturbation velocities are induced by linear internal source and vorticity distributions on the mean camber line of the airfoil and nonlinear field source distributions external to the airfoil surface. Derivatives are calculated in the computational plane, and those in the physical plane are determined by using the Jacobian of the transformation. An O-type grid is applied to reduce the numerical errors in the region close to the location where the shock wave occurs. The calculations have been carried out for NACA 0012, parabolic arc, and circular arc airfoils at various subcritical freestream Mach numbers. The results of the present method are compared with earlier results and are shown to be in good agreement.

Nomenclature

a	= local speed of sound
J	= Jacobian of the transformation
M_∞	= freestream Mach number
T	= artificial viscosity
u,v	= total velocity components in x and y axes
u_∞,v_∞	= freestream velocity components in x and y axes
W	= weighting function
z	= $(x + iy)$ coordinates in physical planes
α	= angle of incidence
β	= vorticity strength
γ	= ratio of specific heats (= 1.4 for air)
δ	= thickness ratio of airfoil
μ	= switching function
ρ	= air density
σ	= source strength
σ_f	= field source strength
ϕ	= perturbation velocity potential

Subscripts

r,θ	= derivatives in r and θ directions
x,y	= derivatives in x and y directions
∞	= freestream

Introduction

THE integral equation method is one of the oldest methods for calculating transonic flows. The recent reviews of the application of the integral equation method to small perturbation transonic flows are given by Spreiter[1] and Niyogi.[2] Ravichandran et al.[3] used the internal singularity model, i.e., one of the integral equation methods in which the singularity is placed on the mean camber line of the airfoil, and finite difference formulas to solve transonic full-potential flow. However, Sinclair[4] applied the surface singularity model, i.e., the singularity is placed on the airfoil surface and difference formulas to solve transonic full-potential flow. Ogana[5] as well as Ogana and Spreiter[6] gave the derivation of the singularity kernel for the integral equation method. Nixon[7] developed an alternative means to evaluate the field integral.

In this paper, the integral equation method, in which the singularities of source and vorticity are linearly distributed on the mean camber line of the airfoil, is modified and applied to compute full-potential solutions for transonic flows over airfoils with embedded supersonic regions. The integral equation method for the present approach was developed by Chen and Sheu.[8,9] The method for the approach of Ravichandran et al. was developed by Basu.[10] The disadvantage for the model developed by Basu can be found in Ref. 9. The calculations have been carried out for three test airfoils, i.e., NACA 0012, parabolic arc, and circular arc airfoils. The results of the present method are compared to those given by earlier numerical computation and experimental data.

Mathematical Analysis

The potential equation in steady, inviscid, compressible, and two-dimensional flow past an arbitrary body can be written as

$$(a^2 - u^2)\phi_{xx} - 2uv\phi_{xy} + (a^2 - v^2)\phi_{yy} = 0 \tag{1}$$

where

$$u = u_\infty + \phi_x, \qquad v = v_\infty + \phi_y, \qquad q^2 = u^2 + v^2$$

The energy equation is

$$a^2 = (1/M_\infty^2) + [(\gamma - 1)/2](1 - q^2) \quad \text{and} \quad \gamma = 1.4 \tag{2}$$

Equation (1) can be written as

$$\phi_{xx} + \phi_{yy} = \sigma_f \tag{3a}$$

where

$$\sigma_f = (u^2/a^2)\phi_{xx} + (2uv/a^2)\phi_{xy} + (v^2/a^2)\phi_{yy} \tag{3b}$$

Thus, the velocity components in the x and y directions at a field point (x,y) can be expressed as the sum of the velocity induced by the internal singularities on the mean camber line

Received May 30, 1989; revision received Feb. 16, 1990. Copyright © 1990 by the American Institute of Aeronautics and Astronautics, Inc. All rights reserved.

*Postgraduate Student, Department of Power Mechanical Engineering.

†Associate Professor, Department of Power Mechanical Engineering; currently, Project Manager, Optimal Computer Aided Engineering, Inc., Novi, MI. Member AIAA.

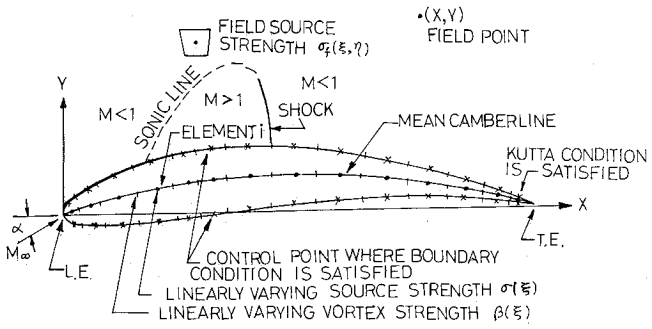

Fig. 1 Numerical model for airfoil in compressible flows.

of the airfoil, the field source σ_f, and the freestream velocity, i.e.,

$$u = u_\infty + \int_c \frac{\sigma}{2\pi} K_1 \, d\xi + \int_c \frac{\beta}{2\pi} K_2 \, d\xi + \iint_f \frac{\sigma_f}{2\pi} K_3 \, d\xi \, d\eta \quad (4a)$$

$$v = v_\infty + \int_c \frac{\sigma}{2\pi} K_2 \, d\xi - \int_c \frac{\beta}{2\pi} K_1 \, d\xi + \iint_f \frac{\sigma_f}{2\pi} K_4 \, d\xi \, d\eta \quad (4b)$$

where curve c denotes the mean camber line of airfoil and f denotes the region external to the airfoil contour. The σ and β are the linear distributions of source and vorticity strengths on the mean camber line of the airfoil, and σ_f is the uniform distribution of field source strength on the small element in region f (see Fig. 1);

$$K_1 = \frac{x-\xi}{(x-\xi)^2+y^2} \qquad K_2 = \frac{y}{(x-\xi)^2+y^2}$$

$$K_3 = \frac{x-\xi}{(x-\xi)^2+(y-\eta)^2} \qquad K_4 = \frac{y-\eta}{(x-\xi)^2+(y-\eta)^2}$$

The O-type grid generation given by Inoue[11] is used to provide a smooth body fitted system of grid lines. The function that maps conformally the region exterior to the airfoil section onto the exterior of the unit circle is determined in an explicit form, and the mesh spacing can be controlled. The O-type grid obtained by the present method is shown in Fig. 2. All of the derivatives in the computational plane (i.e., ζ plane) are calculated by finite differences, and those of the physical plane (i.e., Z plane) are given by using the Jacobian of the transformation. Equation (3b) can be rewritten as

$$\sigma_f = (u^2/a^2)u_x + (2uv/a^2)u_y + (v^2/a^2)v_y \quad (5)$$

where

$$u_x = \frac{\partial u}{\partial x} = u_r r_x + u_\theta \theta_x \qquad v_y = \frac{\partial v}{\partial y} = v_r r_y + v_\theta \theta_y$$

$$u_y = \frac{\partial u}{\partial y} = u_r r_y + u_\theta \theta_y \qquad v_x = \frac{\partial v}{\partial x} = \frac{\partial u}{\partial y} = u_y$$

$$J = \begin{bmatrix} r_x & r_y \\ \theta_x & \theta_y \end{bmatrix}$$

In order to achieve convergence for strong supercritical flows, the artificial viscosity suggested by Jameson[12] is used in the present approach. The field source term becomes

$$\sigma_f^* = \sigma_f + T \quad (6)$$

where T is the artifical viscosity and is equal to $(-\partial/\partial s)(\Delta s \, \mu\rho\sigma_f)$, Δs the small element in the streamwise direction, μ the switching function defined by $\mu = \max[0, 1 - a^2/q^2]$, and ρ the density and equal to $(a^2 M_\infty^2)^{1/(\gamma-1)}$.

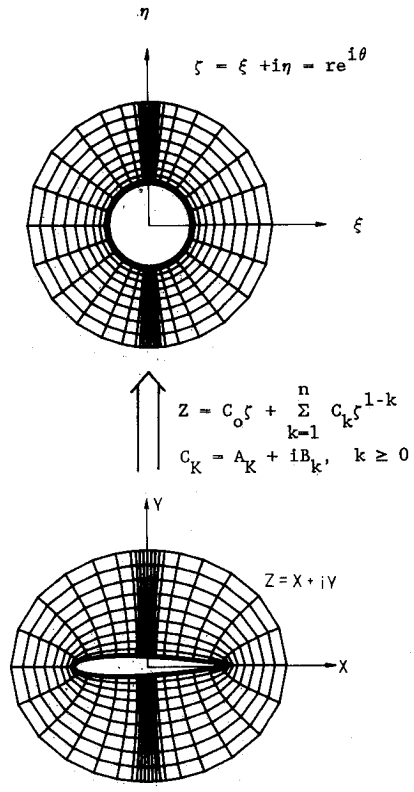

Fig. 2 O-type grid generation.

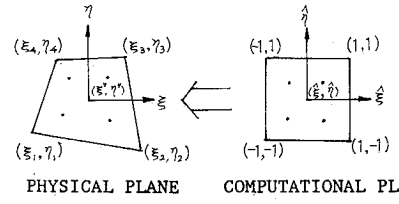

Fig. 3 Four-node quadrilateral finite element transformation.

In order to reduce the truncation errors for the double integral of the field source term in Eq. (4), the four-node quadrilateral finite element is used to transform a quadrilateral element in the physical plane (ξ,η) to a square element in the computational plane $(\hat{\xi},\hat{\eta})$ (see Fig. 3). The function of the transformation is given by

$$\xi^* = \sum_{i=1}^{4} \xi_i g_i(\hat{\xi}_i,\hat{\eta}_i)$$

$$\eta^* = \sum_{i=1}^{4} \eta_i g_i(\hat{\xi}_i,\hat{\eta}_i) \quad (7)$$

where

$$g_1 = (1/4)(1-\hat{\xi}_1)(1-\hat{\eta}_1) \qquad g_2 = (1/4)(1+\hat{\xi}_2)(1-\hat{\eta}_2)$$

$$g_3 = (1/4)(1+\hat{\xi}_3)(1+\hat{\eta}_3) \qquad g_4 = (1/4)(1-\hat{\xi}_4)(1+\hat{\eta}_4)$$

Thus, the double integral is written as

$$\iint_\Omega f(\xi,\eta) \, d\xi \, d\eta = \iint_{\hat{\Omega}} f(\hat{\xi},\hat{\eta}) J(\hat{\xi},\hat{\eta}) \, d\hat{\xi} \, d\hat{\eta}$$

$$= \sum_{i=1}^{4} f(\hat{\xi}_i,\hat{\eta}_i) J(\hat{\xi}_i,\hat{\eta}_i) W_i \quad (8)$$

where

$$J(\hat{\xi},\hat{\eta}) = \frac{\partial\xi}{\partial\hat{\xi}}\frac{\partial\eta}{\partial\hat{\eta}} - \frac{\partial\xi}{\partial\hat{\eta}}\frac{\partial\eta}{\partial\hat{\xi}}$$

and the weighting function $W_i = 1.0$, $i = 1,2,3,4$, for a four-point quadrature rule of Gauss integration:

$$(\hat{\xi}_1,\hat{\eta}_1) = [(-1/\sqrt{3}),(-1/\sqrt{3})] \qquad (\hat{\xi}_3,\hat{\eta}_3) = [(1/\sqrt{3}),(1/\sqrt{3})]$$

$$(\hat{\xi}_2,\hat{\eta}_2) = [(1/\sqrt{3}),(-1/\sqrt{3})] \qquad (\hat{\xi}_4,\hat{\eta}_4) = [(-1/\sqrt{3}),(1/\sqrt{3})]$$

The iterative scheme for the present method is described in the following.

1) The internal singularities of source and vorticity linearly distributed on the mean camber line of the airfoil are obtained by satisfying the boundary condition of tangential flow over the airfoil surface and Kutta condition of no loading at the trailing edge of the airfoil. It is assumed that the strength of field source is zero for the first iteration.

2) The velocity components of u and v and the derivatives of velocity (i.e., u_x, u_y, v_x, and v_y) at field control points are calculated by the contributions of the strengths of internal singularities that are provided by step 3 (using step 1 on the first iteration). The contributions to these values are added to the previous solutions, which are given by the previous field source strengths. As the values of derivatives at all field control points are determined, the strengths of the field source at the control points are obtained from Eq. (3b).

3) The new internal singularities of source and vorticity linearly distributed on the mean camber line of the airfoil are determined by satisfying the boundary condition and the Kutta condition due to the contributions of freestream velocity and new field source strength given by step 2.

4) Repeat steps 2 and 3 until convergence of the field source strengths in step 2 is achieved within the error of tolerance 3×10^{-3}.

Results and Discussions

The examples have been carried out using NACA 0012, parabolic arc, and circular arc airfoils for which subcritical and supercritical results are available for comparison.

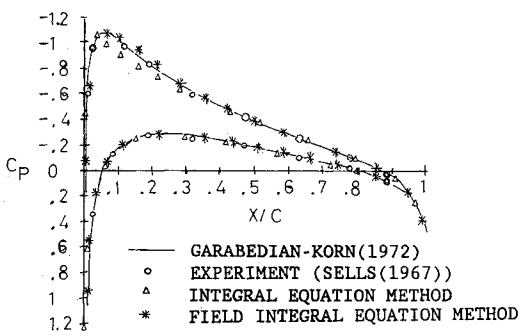

Fig. 4 Subcritical pressure distribution on NACA 0012 airfoil; $M_\infty = 0.63$, $\alpha = 2$ deg, 40 surface elements.

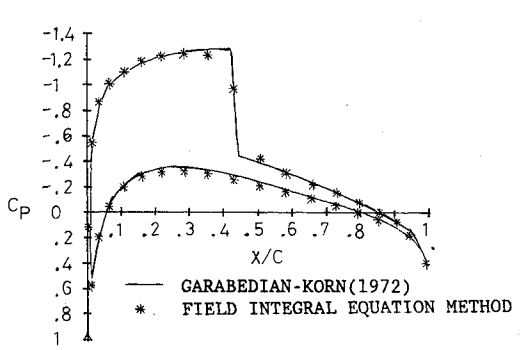

Fig. 5 Supercritical pressure distribution on NACA 0012 airfoil; $M_\infty = 0.75$, $\alpha = 2$ deg, 40 surface elements.

Figure 4 shows the pressure distribution on a NACA 0012 airfoil for a subcritical lifting case run at a freestream Mach number M_∞ of 0.63 and an incidence α of 2 deg. The results of the field integral equation method are calculated by using 20 elements on the mean camber line of airfoil, i.e., a total of 40 elements on the surface of airfoil. A nonuniform field mesh of 50×12 is used with the finer mesh close to the region where the shock wave shows up, extending 0.5 chord distance from both the leading edge and the trailing edge of the airfoil. The Garabedian et al.[13] results were calculated on a grid of 160×30. The results for the integral equation method are obtained by an improved compressibility correction with the modification to the Prandtl-Glauert rule. The agreement between the results of the field integral equation method, the integral equation method, those of Garabedian et al.,[13] and the experimental data of Sells[14] is very good.

Figure 5 presents the pressure distribution over a NACA 0012 airfoil with $M_\infty = 0.75$ and $\alpha = 2$ deg. Because the integral equation method has no mechanism to predict the shock wave, the result of the integral equation method is not given in Fig. 5. It is seen that the agreement between the results of the field integral equation method and those of Garabedian et al.[13] is good. For the subcritical and supercritical test cases, convergent solutions were obtained in about six iterations.

The computed surface pressure distribution on a NACA 0012 airfoil at $M_\infty = 0.7$ and $\alpha = 2$ deg is shown in Fig. 6. The results of the field integral equation method agree well with those obtained by Cole and Cook.[15] Figure 7 gives the pressure distribution on a NACA 0012 airfoil at $M_\infty = 0.8$ and $\alpha = 0$ deg. The agreement between the results calculated by the present method and those of the numerical computation given by Baker,[16] and the experimental data of Bailey[17] is seen to be rather good.

A subcritical pressure distribution on a 10% thick parabolic arc biconvex airfoil at $M_\infty = 0.7$ and $\alpha = 0$ deg is shown in Fig. 8. The results of a numerical solution supplied by Martin and Lomax[19] are compared with those given by the present numerical method. The transonic similarity parameter K was proposed by Spreiter,[18] i.e., $K = (1 - M_\infty^2)/(M_\infty^2\,\delta)^{2/3}$, where δ is the thickness ratio of airfoil.

Figure 9 presents the pressure distribution for a 6% thick parabolic arc biconvex airfoil at $M_\infty = 0.909$ and $\alpha = 0$ deg.

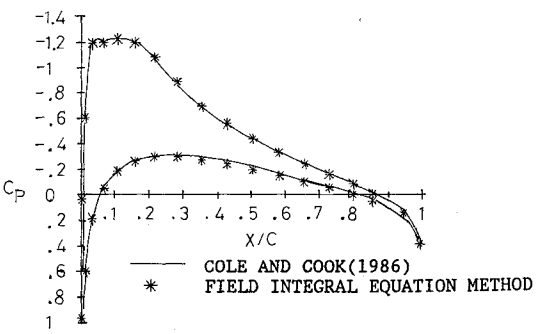

Fig. 6 Supercritical pressure distribution on NACA 0012 airfoil; $M_\infty = 0.7$, $\alpha = 2$ deg, 40 surface elements.

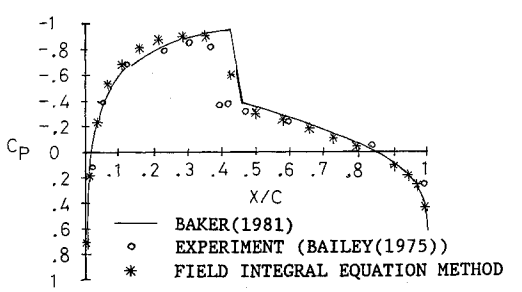

Fig. 7 Supercritical pressure distribution on NACA 0012 airfoil; $M_\infty = 0.8$, $\alpha = 0$ deg, 40 surface elements.

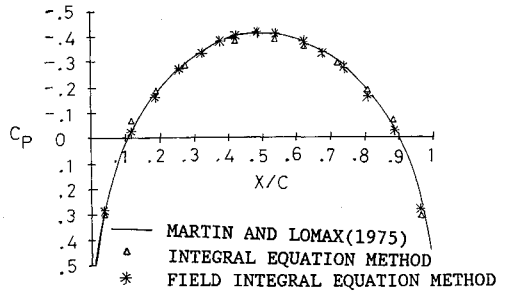

Fig. 8 Subcritical pressure distribution on 10% thick parabolic arc airfoil; $M_\infty = 0.7$, $\alpha = 0$ deg, $k = 3.81$, 40 surface elements.

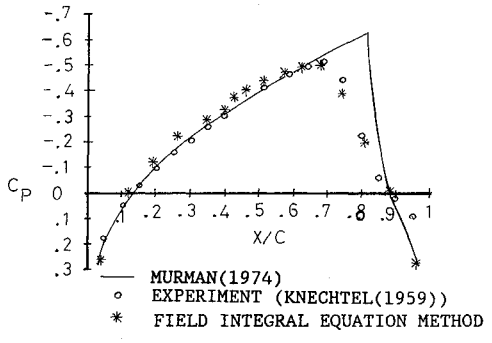

Fig. 9 Supercritical pressure distribution on 6% thick parabolic arc airfoil; $M_\infty = 0.909$, $\alpha = 0$ deg, $k = 1.29$, 40 surface elements.

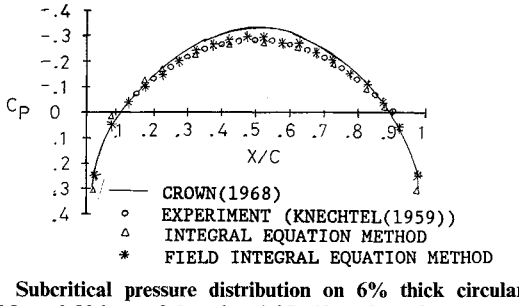

Fig. 10 Subcritical pressure distribution on 6% thick circular arc airfoil; $M_\infty = 0.806$, $\alpha = 0$ deg, $k = 3.05$, 40 surface elements.

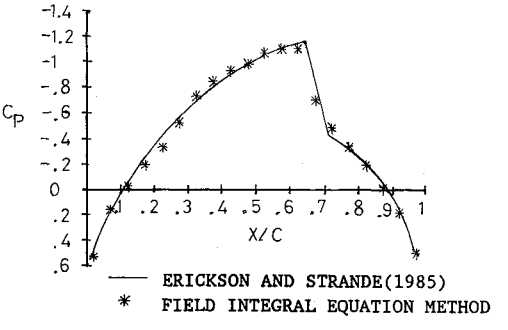

Fig. 11 Supercritical pressure distribution on 18% thick circular arc airfoil; $M_\infty = 0.73$, $\alpha = 0$ deg, $k = 2.23$, 40 surface elements.

The agreement between the results of the field integral equation method and those of the experimental data of Knechtel[21] is very good; however, the numerical solution using the relaxation method given by Murman[20] gives a location of shock wave aft to the experimental data.

Figure 10 gives the subcritical pressure distribution on a 6% thick circular arc biconvex airfoil at $M_\infty = 0.806$ and $\alpha = 0$ deg. The results of the field integral equation method are closer to the experimental data of Knechtel[21] than those of the numerical solutions obtained by Crown.[22] The pressure distribution on a 18% thick circular arc biconvex airfoil at $M_\infty = 0.73$ and $\alpha = 0$ deg is shown in Fig. 11. The present solutions agree well with the numerical solutions of the Pan Air computer code, which were given in Erickson and Strande.[23]

Conclusions

A field integral equation method that combines the integral equation method and the finite-difference method has been developed to solve a NACA 0012 airfoil and a biconvex airfoil at several angles of incidence and various transonic Mach numbers by satisfying the tangency boundary conditions on the airfoil surface. The present approach is able to capture the shocks over a few mesh widths whose strengths and locations agree well with the results of finite-difference calculations. It shows that the use of an incompressible integral equation model with the addition of artificial viscosity to the governing equation is able to produce convergent solutions for most cases arising in inviscid flows with shocks. This method has good results compared to the finite-difference grids even with the coarse grids.

In the present approach, the mean camber line was divided into 20 elements and the field external to the airfoil was divided into 50 × 12 elements. The convergent solutions could be obtained using various grid points on the mean camber line and field grid system. The grid need not extend to a very far field, i.e., only encompassing the regions of compressibility. The total field grid points required in the present method could be reduced much more than those used in the calculation of finite-difference methods. Moreover, the present internal singularity model can be applied to any airfoils without the disadvantages of the model developed by Basu.

References

[1]Spreiter, J. R., "Transonic Aerodynamics—History and Statement of the Problem," *Transonic Aerodynamics,* Vol. 81, Progress in Astronautics and Aeronautics, edited by D. Nixon, AIAA, New York, 1981, pp. 3–79.

[2]Niyogi, P., "Integral Equation Method in Transonic Flow," *Lecture Notes in Physics*, Vol. 157, Springer-Verlag, New York, 1982.

[3]Ravichandran, K. S., Arora, N. L., and Singh, R., "Transonic Full Potential Solutions by An Integral Equation Method," *AIAA Journal*, Vol. 22, No. 6, 1983, pp. 882–888.

[4]Sinclair, P. M., "An Exact Integral (Field Panel) Method for the Calculation of Two-Dimensional Transonic Potential Flow Around Complex Configurations," *Aeronautical Journal*, June/July 1986, pp. 227–236.

[5]Ogana, W., "Numerical Solution for Subcritical Flows by a Transonic Integral Equation Method," *AIAA Journal*, Vol. 15, No. 3, 1977, pp. 444–446.

[6]Ogana, W., and Spreiter, J. R., "Derivation of an Integral Equation for Transonic Flows," *AIAA Journal*, Vol. 15, No. 2, 1977, pp. 281–283.

[7]Nixon, D., "Extended Integral Equation Method for Transonic Flows," *AIAA Journal*, Vol. 13, No. 7, 1975, pp. 934–935.

[8]Chen, D. R., and Sheu, M. J., "Comparison of Numerical Solutions of Lower and Higher Order Integral Equation Methods for Two-Dimensional Aerofoils," AIAA Paper 86-2591, 1986.

[9]Chen, D. R., and Sheu, M. J., "Investigation of Numerical Solution of Integral Equation Methods for Multi-Element Aerofoils," *Computer Methods in Applied Mechanics and Engineering*, Vol. 68, No. 3, 1988, pp. 345–364.

[10]Basu, B. C., "A Mean Camber Line Singularity Method for Two-Dimensional Steady and Oscillatory Aerofoils and Control Surface in Inviscid, Incompressible Flow," Aeronautical Research Council, ARC CP 1391, Oct. 1976.

[11]Inoue, K., "Grid Generation for Single Airfoil Using Conformal Mapping," National Aerospace Laboratory, Japan, TR-851T, 1984, pp. 1–4.

[12]Jameson, A., "Transonic Potential Flow Calculations Using Conservation Form," *Proceedings of 2nd AIAA Conference on Computational Fluid Dynamics*, AIAA, New York, June 1975, pp. 148–161.

[13]Garabedian, P., Korn, D. G., and Jameson, A., "Supercritical Wing Sections," *Lecture Notes in Economic and Mathematical Systems*, Springer-Verlag, New York, No. 66, 1972.

[14]Sells, C. C. L., "Plane Subcritical Flow Past A Lifting Airfoil,"

Royal Aircraft Establishment, England, RAE TR-67146, 1967.

[15]Cole, J. D., and Cook, L. P., "Transonic Aerodynamics," *Applied Mathematics and Mechanics,* North Holland, New York, Vol. 30, 1986, p. 317.

[16]Baker, T. J., "The Computation of Transonic Potential Flow," *Computational Methods for Turbulent, Transonic and Viscous Flows*, edited by J. A. Essers, Hemisphere, New York, 1983.

[17]Bailey, F. R., "On the Computation of Two- and Three-Dimensional Steady Transonic Flows by Relaxation Methods," *Lecture Notes in Physics*, Vol. 41, edited by H. J. Wirz, 1975, pp. 1–77.

[18]Spreiter, J., "On the Application of Transonic Similarity Rules to Wings of Finite Span," NACA TR 1153, 1953.

[19]Martin, E. D., and Lomax, H., "Rapid Finite Difference Computation of Subsonic and Slightly Supercritical Aerodynamic Flows," *AIAA Journal*, Vol. 13, No. 5, 1975, pp. 579–586.

[20]Murman, E. M., "Analysis of Embedded Shock Waves Calculated by Relaxation Methods," *AIAA Journal*, Vol. 12, No. 5, 1974, pp. 626–633.

[21]Knechtel, E. D., "Experimental Investigations at Transonic Speeds of Pressure Distribution over Wedge and Circular Arc Airfoil Sections and Evaluation of NASA Perforated Wall Interference," NASA TN D-15, 1959.

[22]Crown, J. C., "Calculation of Transonic Flow Over Thick Airfoils by Integral Methods," *AIAA Journal*, Vol. 6, No. 3, 1968, pp. 413–423.

[23]Erickson, L. L., and Strande, S. M., "A Theoretical Basis for Extending Surface Paneling Methods to Transonic Flow," *AIAA Journal*, Vol. 23, No. 12, 1985, pp. 1860–1867.

Attention Journal Authors: Send Us Your Manuscript Disk

AIAA now has equipment that can convert **virtually any disk** (3½-, 5¼-, or 8-inch) **directly to type**, thus avoiding rekeyboarding and subsequent introduction of errors.

The following are examples of easily converted software programs:

- PC or Macintosh TEX and LATEX
- PC or Macintosh Microsoft Word
- PC Wordstar Professional

You can help us in the following way. If your manuscript was prepared with a word-processing program, please *retain the disk* until the review process has been completed and final revisions have been incorporated in your paper. Then send the Associate Editor *all* of the following:

- Your final version of double-spaced hard copy.
- Original artwork.
- A *copy* of the revised disk (with software identified).

Retain the original disk.

If your revised paper is accepted for publication, the Associate Editor will send the entire package just described to the AIAA Editorial Department for copy editing and typesetting.

Please note that your paper may be typeset in the traditional manner if problems arise during the conversion. A problem may be caused, for instance, by using a "program within a program" (e.g., special mathematical enhancements to word-processing programs). That potential problem may be avoided if you specifically identify the enhancement and the word-processing program.

In any case you will, as always, receive galley proofs before publication. They will reflect all copy and style changes made by the Editorial Department.

We will send you an AIAA tie or scarf (your choice) as a "thank you" for cooperating in our disk conversion program. Just send us a note when you return your galley proofs to let us know which you prefer.

If you have any questions or need further information on disk conversion, please telephone Richard Gaskin, AIAA Production Manager, at (202) 646-7496.

AIAA